oscillations in parotid acinar cells drive oscillations of secretion, $[Cl^-]_i$, $[Na^+]_i$, $[K^+]_i$, and cell volume. The temporal relations and $[Ca^{2+}]_i$ dependencies demonstrate that $[Ca^{2+}]_i$ is the primary signaling mechanism for these oscillations. Nevertheless, an issue to consider is whether oscillating concentrations of intracellular ions or water content are themselves regulatory signals. Our results suggest intracellular cation composition, modulated by $[Ca^{2+}]_i$ oscillations, may in turn modulate $[Ca^{2+}]_i$ oscillations. Oscillating concentrations of monovalent ions may cause the activities of transporters for which they are substrates to oscillate as well. For energy-dependent pumps (for example, the Na^+,K^+-ATPase), oscillations in their activities may result in oscillations of $[ATP]_i$ and cellular metabolism (*17*), which then may affect many cellular processes.

REFERENCES AND NOTES

1. M. J. Berridge, *J. Biol. Chem.* **265**, 9583 (1990); R. Jacob, *Biochim. Biophys. Acta* **1052**, 427 (1990).
2. J. K. Foskett and J. E. Melvin, *Science* **244**, 1582 (1989).
3. J. K. Foskett, C. Roifman, D. Wong, *J. Biol. Chem.* **266**, 2778 (1991).
4. J. K. Foskett and D. Wong, *Am. J. Physiol.*, in press.
5. ———, *J. Biol. Chem.* **266**, 14535 (1991).
6. Exposure of single parotid acinar cells to 2 μM TG plus 10 mM caffeine is the most reliable method to induce $[Ca^{2+}]_i$ oscillations (*5*). These oscillations are indistinguishable from those induced by TG alone.
7. J. K. Foskett, *Am. J. Physiol.* **259**, C998 (1990).
8. K. R. Lau, J. W. Howorth, R. M. Case, *J. Physiol. (London)* **425**, 407 (1990); R. J. Turner, J. N. George, B. J. Baum, *J. Membr. Biol.* **94**, 143 (1986); J. H. Poulsen and B. Nauntofte, *J. Dent. Res.* **66**, 608 (1987); R. Case, M. Hunter, I. Novak, J. A. Young, *J. Physiol. (London)* **349**, 619 (1984); L. H. Smaje, J. H. Poulsen, H. H. Ussing, *Pfluegers Arch.* **406**, 492 (1986).
9. S. P. Soltoff, M. K. McMillian, L. C. Cantley, E. J. Cragoe, Jr., B. R. Talamo, *J. Gen. Physiol.* **93**, 285 (1989); D. Pirani, A. R. Evans, D. I. Cook, J. A. Young, *Pfluegers Arch.* **408**, 178 (1987); S. Dissing and B. Nauntofte, *Am. J. Physiol.* **259**, G1044 (1990).
10. J. E. Melvin, A. Moran, R. J. Turner, *J. Biol. Chem.* **263**, 19564 (1988); M. Manganel and R. J. Turner, *ibid.* **265**, 4284 (1990); *J. Membr. Biol.* **111**, 191 (1989); J. R. Martinez, S. Barker, J. Camden, *Eur. J. Pharmacol.* **164**, 335 (1989); M. C. Steward, Y. Seo, R. M. Case, *Pfluegers Arch.* **414**, 200 (1989); I. Novak and J. A. Young, *ibid.*, p. 68.
11. A. Minta and R. Y. Tsien, *J. Biol. Chem.* **264**, 19449 (1989).
12. Intracellular SBFI fluorescence was diffusely distributed and concentrated in vesicular compartments. Extent of dye compartmentation was variable among cells and was more pronounced when loading was performed at 37°C. Compartmentalized dye yielded a somewhat higher excitation ratio but was similarly $[Na^+]$-sensitive to the cytoplasm. Because of this, and because the volume of the compartmentalized dye represented a minor fraction of the total cellular volume, we determined $[Na^+]$, by averaging pixel intensities throughout the cell with subsequent conversion by calibrations. We converted intracellular SBFI fluorescence ratios to $[Na^+]$, by exposing cells to various extracellular $[Na^+]$ in the presence of 5 μM gramicidin in the standard medium, except that Cl^- was reduced to 60 mM (gluconate substitution), the $[Cl^-]_i$ in single parotid acinar cells (*7*), to prevent cell swelling. $[Na^+]$ in the bathing medium was altered by isosmotic replacement with K^+. The dissociation constant K_d for the dye was 22 mM. The data fitted reasonably well the equation $[Na^+]_i = K_d B (R - R_0)/(R_{max} - R)$, where R_0 and R_{max} are the measured ratios in the absence and in the presence of saturating (150 mM) intracellular $[Na^+]$, respectively, and B is the ratio of the emission intensities determined at 380-nm excitation for free and bound indicator. B was estimated to be 1.3 and R_{max}/R_0 to be 3.0. The upper limit for accurate $[Na^+]_i$ quantitation was ~80 to 100 mM.
13. The rapid cell shrinkage associated with the large-amplitude $[Ca^{2+}]_i$ spikes was not initially associated with a change in $[Na^+]_i$. A rise of $[Na^+]_i$ by ~20% would be expected on the basis of a 20% cell volume reduction. With average $[Na^+]_i$ ~9 mM, the expected rise in $[Na^+]_i$ would be ~1.8 mM, which is just at the level of resolution in our system.
14. Near saturation of the dye by $[Na^+]$ higher than ~100 mM limited our ability to resolve the $[Na^+]_i$ reached during some $[Na^+]_i$ transients associated with $[Ca^{2+}]_i$ oscillations. To compute the statistics, we assumed that $[Na^+]_i$ reached in these cells during such transients (nine out of 55 cells) was 100 mM. Similarly, during ouabain inhibition $[Na^+]_i$ usually rose to concentrations that were not resolvable with the dye.
15. M. Wong and J. K. Foskett, unpublished data.
16. In most cells, intracellular osmolarity is determined by the sum of the concentrations of Na^+, K^+, Cl^-, and impermeant anionic macromolecules (A^-). Because highly water-permeable cell membranes ensure that intracellular osmolarity equals that of the extracellular medium, and preservation of electrical neutrality dictates that $[Na^+]_i + [K^+]_i = [Cl^-]_i + [A^-]_i$, it follows that $[Na^+]_i + [K^+]_i$ contributes half of the cellular osmolarity. Our experiments were performed in isosmotic media; consequently, $[Na^+]_i + [K^+]_i$ always equals ~150 mM, regardless of the cell volume at different times in the oscillation cycle. Calculations of changes in intracellular Na^+ and K^+ contents, from $[Na^+]_i$ and $[K^+]_i$ and cell volume, indicate that neither Na^+ content, K^+ content, nor their sum, are constant during the oscillations. A detailed analysis of the changes in ion concentrations and contents during oscillations is in preparation.
17. Phospholipase C–mediated agonists, the Ca^{2+} ionophore ionomycin, and nystatin (to increase Na^+ entry) each greatly increases O_2 consumption in salivary acinar cells, which are entirely ouabain-sensitive [S. P. Soltoff *et al.*, in (*9*)].
18. J. K. Foskett, *Am. J. Physiol.* **255**, C566 (1988).

19. Supported by the Canadian Cystic Fibrosis Foundation (CCFF). M.M.Y.W. is a CCFF predoctoral fellow. J.K.F. is a CCFF scholar. We thank Q. Liu for technical assistance and S. Grinstein for comments.

20 June 1991; accepted 23 August 1991

GPI-Anchored Cell-Surface Molecules Complexed to Protein Tyrosine Kinases

IRENA STEFANOVÁ,*† VÁCLAV HOŘEJŠÍ, IGNACIO J. ANSOTEGUI, WALTER KNAPP, HANNES STOCKINGER

Binding of ligand or antibody to certain cell-surface proteins that are anchored to the membrane by glycophosphatidylinositol (GPI) can cause activation of leukocytes. However, it is not known how these molecules, which lack intracellular domains, can transduce signals. The GPI-linked human molecules CD59, CD55, CD48, CD24, and CD14 as well as the mouse molecules Thy-1 and Ly-6 were found to associate with protein tyrosine kinases, key regulators of cell activation and signal transduction. A protein tyrosine kinase associated with the GPI-linked proteins CD59, CD55, and CD48 in human T cells, and with Thy-1 in mouse T cells was identified as $p56^{lck}$, a protein tyrosine kinase related to Src. This interaction of GPI-linked molecules with protein tyrosine kinases suggests a potential mechanism of signal transduction in cells.

A VARIETY OF CELL-SURFACE PROTEINS are anchored in the membrane by glycophosphatidylinositol (GPI) (*1*). Some of these molecules are involved in cell adhesion or regulation of the complement system, but the physiological functions of most of them are unknown (*2*). Binding of natural ligands or antibodies to some GPI-linked proteins induces leukocyte activation (*3*). To explore the signal-transducing capacity of GPI-linked molecules, we studied transmembrane and intracellular molecules that are associated with them.

Many receptors have intrinsic or associated protein tyrosine kinase (PTK) activities that are required for signal transduction (*4*). Therefore, we analyzed phosphotransferase activity in immunoprecipitates of various GPI-anchored molecules. Protein kinase activity was co-precipitated with the GPI-linked human molecules CD59 (homologous restriction factor 20), CD55 (decay-accelerating factor), and CD48 from various types of cells, CD24 from B-chronic lymphoblastic leukemia (B-CLL) cells, CD14 from monocytes, and Thy-1 and Ly-6 from mouse cell lines (Fig. 1). In contrast, no protein kinase activity was detected in association with several other molecules that are anchored in the membrane of these cells

I. Štefanová, W. Knapp, H. Stockinger, Institute of Immunology--Vienna International Research Cooperation Center at SFI, University of Vienna, Brunner Strasse 59, A-1235 Vienna, Austria.
V. Hořejší, Institute of Molecular Genetics, Czechoslovak Academy of Sciences, 142 20 Prague 4, Vídeňská 1083, Czechoslovakia.
I. J. Ansotegui, Department of Immunology, Karolinska Institute, S-104 01 Stockholm, Sweden.

*To whom correspondence should be addressed.
†On leave from Institute of Molecular Genetics, Czechoslovak Academy of Sciences, 142 20 Prague 4, Vídeňská 1083, Czechoslovakia.

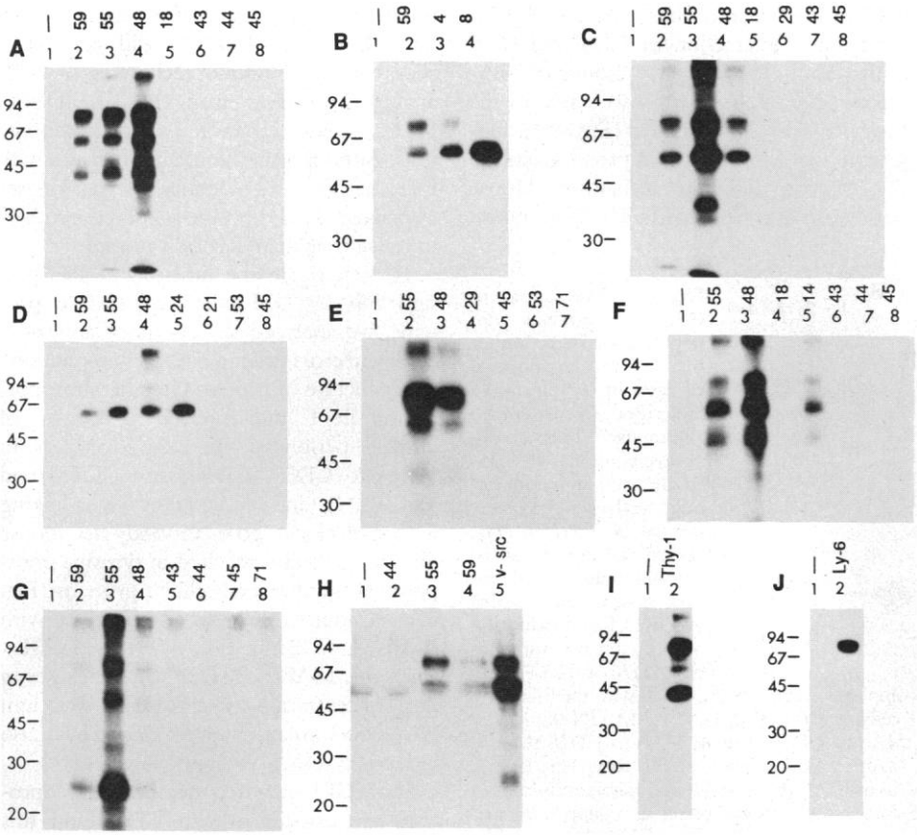

Fig. 1. Co-precipitation of protein kinases with GPI-linked molecules. In vitro kinase assays were performed on immunoprecipitates derived from various cell types (*12*). Complexes were immunoprecipitated with MAb to insulin (IN-05) as a negative control (lane 1 of each gel) or MAb to the cell-surface molecules indicated; CD numbers are shown above the appropriate lanes. The MAbs used in this and other figures (unless otherwise noted) were MAb to CD59 (MEM-43), MAb to CD55 (143-30), MAb to CD48 (34-57, Immunotech), MAb to CD18 (MEM-48), MAb to CD43 (MEM-59), MAb to CD44 (MEM-85), MAb to CD45 (MEM-28), MAb to CD4 (MEM-16), MAb to CD8 (MEM-31), MAb to CD29 (K20), MAb to CD24 (VIBE3), MAb to CD21 (S-B2, Biosys), MAb to CD53 (MEM-53), MAb to CD71 (MEM-75), and MAb to CD14 (MEM-18). (**A**) Human peripheral T lymphocytes. (**B**) Peripheral T lymphocytes lysed in the absence of IAA. The association of $p56^{lck}$ with CD4 and CD8 is sensitive to alkylating agents such as IAA (*8*). Therefore, CD4 and CD8 were precipitated in lysis buffer without IAA. (**C**) Human T cell line HPB-ALL. (**D**) B-CLL cells. (**E**) Human B cell line Daudi. (**F**) Human peripheral monocytes. (**G**) Human myeloid cell line HL-60. (**H**) Human colon carcinoma cell line SW948. Lane 5, MAb to *v-src* (Ab-1, Oncogene); the precipitate of $p60^{c\text{-}src}$ was used as a positive control for the in vitro kinase assay. A similar pattern of phosphorylated molecules was observed in immunoprecipitates of CD59 and CD55 from the melanoma cell line WM9 (*15*). (**I**) Mouse T cell line EL-4. Lane 2, MAb to Thy-1 (1aG4). (**J**) Mouse cell line BW5147. Lane 2, MAb to Ly-6 (D7). Molecular size standards are indicated in kilodaltons.

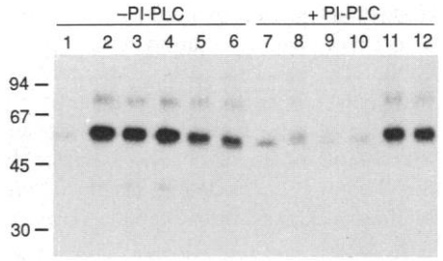

Fig. 2. Effect of treatment of HPB-ALL cells with PI-PLC (Immunotech) on co-precipitation of GPI-linked antigens with protein kinases. PI-PLC treatment was done as described (*14*). Immunoprecipitation and in vitro kinase assay were performed as described (*12*). Lanes 1 to 6, untreated cells; lanes 7 to 12, cells after PI-PLC treatment. Lanes 1 and 7, MAb IN-05; lanes 2 and 8, MAb to CD59; lanes 3 and 9, MAb to CD55; lanes 4 and 10, MAb to CD48; lanes 5 and 11, MAb to CD4; lanes 6 and 12, MAb to CD8. Molecular size standards are indicated in kilodaltons.

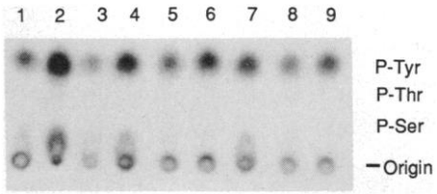

Fig. 3. Phosphoamino acid analysis of proteins co-precipitated with CD55 and labeled in an in vitro kinase assay. Phosphorylated molecules were separated by SDS-PAGE (*12*) and transferred to Immobilon (Millipore) membrane. Phosphoamino acids were eluted from the pieces of Immobilon containing individual phosphoproteins by base and acid hydrolysis (*16*), and analyzed by thin-layer chromatography (*17*) and autoradiography. Analysis of phosphoproteins precipitated by the MAb to CD55 from lysates of the following cell lines: HPB-ALL cells (Fig. 1C, lane 3) lane 1, p80; lane 2, p56; lane 3, p40; lane 4, p35; Daudi cells (Fig. 1E, lane 2) lane 5, p80; lane 6, p60; HL-60 cells (Fig. 1G, lane 3) lane 7, p80; lane 8, p60; and lane 9, p25. Positions of standard phosphoamino acids are indicated. P-Ser, phosphoserine; P-Thr, phosphothreonine; P-Tyr, phosphotyrosine.

through a transmembrane polypeptide (except for CD4 and CD8 in T cells) (Fig. 1).

There is evidence that alternative mRNA processing can lead to co-expression of another form of these cell-surface proteins with a hydrophobic transmembrane polypeptide and cytoplasmic domain (*5*). To determine if these putative non-GPI–linked forms are responsible for association with protein kinases, we removed GPI-linked proteins from the surface of cells from the human T cell line HPB-ALL by treating the cells with GPI-specific phospholipase C (PI-PLC) before immunoprecipitation. Under these conditions, phosphorylation in the immunoprecipitates of CD48, CD55, and CD59 was nearly completely abolished (Fig. 2), but the amount of phosphorylation in immunoprecipitates of CD4 and CD8 was not reduced. Thus, intact GPI-linked proteins appear to be required for association with protein kinases.

In vitro phosphorylation of proteins co-precipitated with CD55 from HPB-ALL, Daudi, and HL60 cells resulted in labeling exclusively on tyrosine residues (Fig. 3). Specific tyrosine phosphorylation was also observed in the immunoprecipitates of CD55 and CD59 from the SW948 colon carcinoma and WM9 melanoma cell lines, CD24 from B-CLL cells, CD14 from monocytes, as well as Thy-1 and Ly-6 from the EL-4 and BW5147 mouse cell lines, respectively.

The patterns of the proteins phosphorylated in vitro in the CD4, CD8, and CD59 immunoprecipitates were similar (Fig. 1B). The CD4 and CD8 glycoproteins are known to be physically associated with the PTK $p56^{lck}$ (*6*). We detected $p56^{lck}$ in immunoprecipitates of CD59, CD55, and CD48 from T cells by immunoblotting with a monoclonal antibody (MAb) to $p56^{lck}$, 1B3 (7) (Fig. 4A). Furthermore, digestion of $p56^{lck}$ (isolated by association with CD4) and the 56-kD phosphoprotein associated with CD59 with protease from *Staphylococcus aureus* strain V8 (V8 protease) yielded identical peptides (Fig. 4B). The CD4 protein was not detected in the complex immunoprecipitated with CD59 from HPB-ALL cells, and no CD59 antigen co-precipitated with CD4 and CD8 (Fig. 4C). These results indicate that the association of $p56^{lck}$ with

the GPI-anchored proteins does not occur as a result of their association with CD4 or CD8. The association of CD4 and CD8 with $p56^{lck}$ is critically dependent on the presence of free cysteine residues (*8*), and the complexes are probably stabilized by metal ions (*9*). Alkylating or metal ion–binding reagents [iodoacetamide (IAA) or 1,10-orthophenanthroline, respectively] inhibited the interaction of CD4 and CD8 with $p56^{lck}$. In contrast, binding of GPI-linked proteins to $p56^{lck}$ was stable in the presence of these substances (Fig. 4D), suggesting that the GPI-linked proteins bind to $p56^{lck}$ by a different mechanism. Mouse $p56^{lck}$ was also detected in Thy-1 immunoprecipitates from lysate of the mouse T cell line EL-4 (Fig. 4A). We did not detect $p56^{lck}$ in the immunoprecipitates of GPI-anchored proteins from B-CLL, Daudi, HL60, colon carcinoma, and melanoma cells. Although they contain molecules with PTK activity, the identity of the kinases associated with the GPI-anchored proteins in cells other than T cells is not known.

To investigate the function of PTKs in signaling by GPI-linked cell-surface proteins, we analyzed the effects of antibody-mediated cross-linking of these molecules on the induction of protein tyrosine phosphorylation in T and B cells. Incubation of human peripheral T lymphocytes with MAbs to CD59, CD55, and CD48 (and also CD4) and subsequent cross-linking with polyclonal goat antibody to mouse immunoglobulins resulted in tyrosine phosphorylation of several cellular proteins (Fig. 5A). A similar result was also obtained with MAbs to CD24 in B-CLL cells (Fig. 5B). The same MAbs to CD24 cause changes in the concentration of cytoplasmic calcium (*10*). Cross-linking with MAb to Thy-1 also induced tyrosine phosphorylation (*11*).

Some GPI-anchored membrane glycoproteins are associated with PTKs, and this association may explain the signal-transducing capacity of these molecules. It is not known whether the PTKs interact directly with the glycolipid anchor of the GPI-linked antigens or through interaction with other proteins.

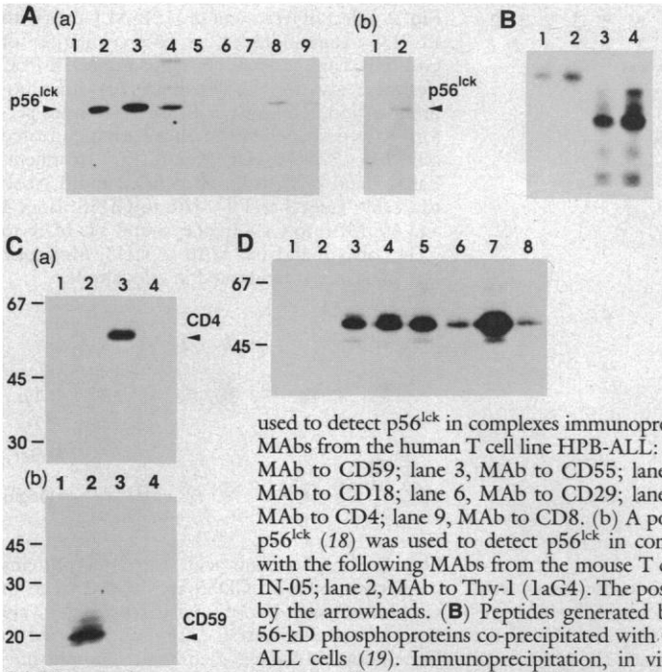

Fig. 4. Association of GPI-linked proteins with $p56^{lck}$. (**A**) Detection of $p56^{lck}$ in immunoprecipitates of GPI-anchored molecules from human and mouse T cells. Immunoprecipitation, SDS-PAGE, and immunoblotting analysis were performed as described (*14*), except that the enhanced chemiluminiscence detection system (Amersham) was used for visualization of proteins on immunoblot. (a) MAb 1B3 (*7*) was used to detect $p56^{lck}$ in complexes immunoprecipitated with the following MAbs from the human T cell line HPB-ALL: Lane 1, MAb IN-05; lane 2, MAb to CD59; lane 3, MAb to CD55; lane 4, MAb to CD48; lane 5, MAb to CD18; lane 6, MAb to CD29; lane 7, MAb to CD43; lane 8, MAb to CD4; lane 9, MAb to CD8. (b) A polyclonal rabbit antiserum to $p56^{lck}$ (*18*) was used to detect $p56^{lck}$ in complexes immunoprecipitated with the following MAbs from the mouse T cell line EL-4: Lane 1, MAb IN-05; lane 2, MAb to Thy-1 (1aG4). The positions of $p56^{lck}$ are indicated by the arrowheads. (**B**) Peptides generated by V8 protease digestion of 56-kD phosphoproteins co-precipitated with CD4 and CD59 from HPB-ALL cells (*19*). Immunoprecipitation, in vitro kinase assay, and SDS-PAGE were done as described (*12*). (**C**) Analysis of co-precipitation of CD59 with CD4 and CD8. Complexes immunoprecipitated with the following MAbs from HPB-ALL cells were analyzed by immunoblotting: Lane 1, MAb IN-05; lane 2, MAb to CD59; lane 3, MAb to CD4; lane 4, MAb to CD8. (a) MAb to CD4 (Leu-3a, Becton Dickinson) was used to detect CD4 on the blot. (b) MAb to CD59 was used to detect CD59 on the blot. Positions of CD4 and CD59 are indicated. (**D**) Stability of the association of CD4, CD8, and CD59 with $p56^{lck}$. Effect of IAA on co-precipitation of $p56^{lck}$. Complexes were immunoprecipitated with the following MAbs from lysates of HPB-ALL cells, and assayed for kinase activity in vitro as described (*12*). Lanes 1, 3, 5, and 7, lysis in the absence of IAA; lanes 2, 4, 6, and 8, lysis in the presence of 5 mM IAA. Lanes 1 and 2, MAb IN-05; lanes 3 and 4, MAb to CD59; lanes 5 and 6, MAb to CD4; lanes 7 and 8, MAb to CD8. The presence of 2 mM 1,10-orthophenanthroline in the lysis buffer did not influence co-precipitation of $p56^{lck}$ with CD59. In contrast, complexes of CD4- and CD8-$p56^{lck}$ were dissociated under these conditions (*20*). Molecular size standards are indicated in kilodaltons.

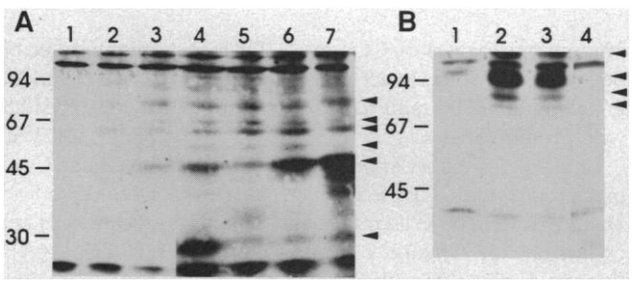

Fig. 5. Phosphorylation of proteins on tyrosine after antibody-mediated cross-linking of GPI-linked molecules in intact cells. Cells were prepared as described (*12*). Cells (1×10^7/ml) were incubated with MAbs (50 μg/ml) for 30 min at 37°C in RPMI 1640 medium, washed and incubated with affinity-purified goat antibody to mouse immunoglobulin (GAM, Sigma) (50 μg/ml) for 20 min at 37°C. Cells were then lysed in lysis buffer (*12*) containing 2 mM Na_2MoO_4 and 2 mM Na_3VO_4. Lysates were mixed with sample buffer and analyzed by SDS-PAGE and immunoblotting as described in Fig. 3. MAb 1G2 (Boehringer Mannheim) was used to detect phosphotyrosine. (**A**) Effect of cross-linking of the following MAbs by GAM on tyrosine phosphorylation in human peripheral T cells. Lane 1, GAM alone; lane 2, MAb to CD18 and GAM; lane 3, MAb to CD4 and GAM; lane 4, MAb to CD55 (BRIC128) and GAM; lane 5, MAb to CD59 (MEM-43) and GAM; lane 6, MAb to CD59 (MEM-129) and GAM; lane 7, MAb to CD48 and GAM. (**B**) Effect of antibody-mediated cross-linking of CD24 molecules on tyrosine phosphorylation in B-CLL cells. Lane 1, GAM alone; lane 2, MAb to CD24 (VIBE3) and GAM; lane 3, MAb to CD24 (VIBC5) and GAM; lane 4, MAb to CD24 (VIBE3) alone. The major substrates for tyrosine phosphorylation are indicated by arrowheads. Molecular size standards are shown in kildaltons.

REFERENCES AND NOTES

1. M. G. Low, *FASEB J.* **3**, 1600 (1989).
2. V. Hořejší, *Adv. Immunol.* **49**, 75 (1991).
3. P. J. Robinson, *Immunol. Today* **12**, 35 (1991).
4. L. C. Cantley *et al.*, *Cell* **64**, 281 (1991).
5. M. G. Low, *Biochim. Biophys. Acta* **988**, 427 (1989).
6. C. E. Rudd, *Immunol. Today* **11**, 400 (1990).
7. I. J. Ansotegui *et al.*, *Scand. J. Immunol.* **33**, 375 (1991).
8. A. S. Shaw *et al.*, *Mol. Cell. Biol.* **10**, 1853 (1990).
9. J. M. Turner *et al.*, *Cell* **60**, 755 (1990).
10. G. F. Fischer, O. Majdic, S. Gadd, W. Knapp, *J. Immunol.* **144**, 638 (1990).
11. E. D. Hsi *et al.*, *J. Biol. Chem.* **264**, 10836 (1989).
12. Peripheral T lymphocytes, monocytes, and B-CLL cells were isolated as described [H. Stockinger *et al.*, *J. Immunol.* **145**, 3889 (1990)]. Cell lines were cultured in RPMI 1640 medium containing fetal calf serum (10%) at 37°C in a 5% CO_2 atmosphere. Cells were solubilized in lysis buffer [10 mM tris-HCl (pH 8.2), 140 mM NaCl, 2 mM EDTA, 1 mM PMSF, 5 mM IAA, aprotinin (10 μg/ml), NP-40 (1%)], and solid phase immunoprecipitation was performed as described (*13*). Immunoprecipitates were incubated with 50 μl of 25 mM Hepes (pH 7.2), containing 3 mM $MnCl_2$, NP-40 (0.1%), and 1 μCi of [γ-^{32}P]ATP (NEN). After incubation for 5 min at 25°C, proteins were eluted in sample buffer and subjected to SDS–polyacrylamide gel electrophoresis (SDS-PAGE) and autoradiography as described (*14*).
13. G. S. Tamura *et al.*, *Anal. Biochem.* **136**, 458 (1984).
14. I. Štefanová *et al.*, *Mol. Immunol.* **26**, 153 (1989).
15. I. Štefanová, V. Hořejší, I. J. Ansotegui, W. Knapp, H. Stockinger, unpublished data.

16. M. P. Kamps and B. M. Sefton, *Anal. Biochem.* **176**, 22 (1989).
17. G. Munoz and S. H. Marshall, *ibid.* **190**, 233 (1990).
18. T. R. Hurley and B. M. Sefton, *Oncogene* **4**, 265 (1989).
19. Phosphorylated polypeptides were localized in the unfixed gel by brief autoradiography. The corresponding zones were cut out, homogenized, and eluted by overnight incubation at 37°C with 10 volumes of a solution containing 0.1 M NH_4HCO_3, 0.1% SDS, 1 mM PMSF, and 5 mM IAA. After addition of BSA (10 μg), the supernatants were lyophilized, and SDS was extracted with methanol. Purified polypeptides were dissolved in 40 μl of 0.1 M tris-HCl (pH 6.8) and incubated for 1 hour at 37°C with V8 protease (0.5 μg) (Boehringer Mannheim). The samples were mixed with an equal volume of sample buffer and analyzed by SDS-PAGE and autoradiography. Lanes 1 and 2, 56-kD polypeptides before V8 treatment; lanes 3 and 4, after V8 treatment. Lanes 1 and 3, 56-kD polypeptide isolated by MAb to CD59 (MEM-43); lanes 2 and 4, 56-kD polypeptide isolated by MAb to CD4 (MEM-16).
20. I. Štefanová, V. Hořejší, I. J. Ansotegui, W. Knapp, H. Stockinger, unpublished data.
21. We thank I. Hilgert and O. Majdic for providing MAbs, D. J. Anstee for MAb to CD55 BRIC128, A. Bernard for MAb to CD29 K20, P. Dráber for MAb to Thy-1 1aG4, B. Sefton for rabbit antiserum to $p56^{lck}$, E. M. Shevach for MAb to Ly-6 D7, and R. Vilella for MAb to CD55 143-30. Supported by the Austrian Research Council, a fellowship from the Sandoz Research Institute Vienna, Austria (I.Š.), and the Swedish Institute and the Swedish Cancer Society (I.J.A.).

28 May 1991; accepted 26 August 1991

Activity-Dependent Synaptic Competition in Vitro: Heterosynaptic Suppression of Developing Synapses

YI-JIUAN LO AND MU-MING POO*

The development and stability of synaptic connections in the nervous system are influenced by the pattern of electrical activity and the competitive interaction between the adjacent nerve terminals. To investigate this influence, a culture system of nerve and muscle cells has been developed in which a single embryonic muscle cell is coinnervated by two spinal neurons. The effect of electrical activity on the synaptic efficacy was examined after repetitive electrical stimulation was applied to one or both neurons. Brief tetanic stimulation of one neuron resulted in immediate functional suppression of the synapse made by the unstimulated neuron innervating the same muscle cell. This heterosynaptic suppression was largely absent when the tetanic stimulation was applied concurrently to both neurons. This result demonstrates that activity-dependent synaptic competition can be studied in vitro at a cellular level.

THE EFFICACY OF SYNAPTIC TRANSmission is susceptible to activity-dependent modulation, a process that underlies much of the plasticity in synaptic function (*1*). In developing nervous systems the pattern of electrical activity also exerts a critical influence on the stabilization and elimination of nerve connections (*2*). In neonatal animals each skeletal muscle fiber is innervated by several axons; all but one are eliminated as the animal matures (*3*). The process of synapse elimination is markedly affected by the activity of the motor nerves (*4*). However, little is known about the cellular mechanisms underlying the activity dependence of synaptic elimination and the nature of competitive interactions among coinnervating nerve terminals. We have designed a cell culture system to study the synaptic physiology associated with the activity-dependent competition between developing neurons.

Cultures of embryonic spinal neurons and myotomal muscle cells were prepared from 1-day-old *Xenopus* embryos (*5*). Functional synaptic contacts between the nerve and muscle cells are established within 24 hours after cell plating (*6*). Experiments were carried out on mononucleated spherical myocytes, which were innervated by two nearby cocultured spinal neurons (see Fig. 1A). The use of the spherical myocyte (average diameter, 35 μm) ensured close proximity of the nerve terminals on the myocyte surface. The synaptic efficacy was examined by whole-cell voltage-clamp recording (*7*) of evoked synaptic currents (ESCs) in the innervated myocyte.

ESCs elicited by the presynaptic neurons were first measured by low-frequency test stimuli. A brief episode of tetanic stimulation was then applied to one neuron, and the synaptic efficacy of both neurons was compared afterward with test stimuli (Fig. 1B). The amplitudes of the ESCs elicited by neurons 1 and 2 averaged 3.4 ± 0.3 (±SEM; $n = 7$) and 1.6 ± 0.4 nA (±SEM; $n = 8$), respectively, at the onset of the experiment. A train of 80 impulses were then elicited in neuron 2 over a period of 40 s. After the stimulus, the synaptic efficacy of neuron 2 increased to an average of 2.6 nA, but that of the unstimulated neuron 1 decreased to 1.7 nA. Over the next 30 min, the ESCs of neuron 1 remained at a suppressed level, while those of neuron 2 remained elevated. Figure 1C depicts the similar change in ESC amplitudes in three such stimulation experiments.

We have performed 13 experiments involving preferential tetanic stimulation. The number of nerve impulses initiated during the tetanus varied between 50 to 100 (at 2 to 5 Hz) (Fig. 2A). In all eight cases where the initial synaptic efficacy was higher at the stimulated synapse (S), significant suppression of the unstimulated synapse (US) was found for all eight synapses within the first 10 min after the tetanic stimulation (rank sum test, $P < 0.05$). In contrast, only one out of eight stimulated synapses showed significant reduction. Significant suppression of unstimulated synapse was also found in three out of five cases where the stimulated synapses had lower initial efficacy. None of the stimulated synapses showed any suppression, and three showed significant potentiation. With the exception of three cases where the suppressed synapse showed substantial recovery of the initial synaptic response with time, persistent suppression was observed for as long as the recording could be made (up to 1 hour; Fig. 2B). The origin of the variability in the extent of suppression among different synapses is unknown. It may be related to the physical proximity of the coinnervating neurites on the muscle surface, which cannot be determined with the phase-contrast optics used here.

In the second series of experiments, the same tetanic stimulation was applied concurrently to both neurons innervating the same myocyte, and the ESCs elicited by each neuron before and after the tetanus were compared. From a total of seven pairs of synapses that were tetanized synchronously (100 pulses, 2 Hz), only three out of 14 synapses showed significant reduction of mean ESC amplitude after the tetani ($P < 0.05$, rank sum test) (Fig. 2A). This result indicates that heterosynaptic suppression is largely absent after synchronous tetanic stimulation. The importance of the synchrony in pre- and postsynaptic activities for protecting the synapse from suppression is illustrated by the experiments in Fig. 3. Simultaneous stimulation (1 + 2) of both neurons produced little or no effect on the ESCs elicited by either neuron, but the same train of stimuli delivered to the neurons asynchronously (1 then 2, with a 100-ms delay between the stimuli applied to the two neurons) resulted in immediate suppression of one or both neurons. Asynchronous tetani often led to asymmetric suppression of the two neurons, as shown in all three cases illustrated. In cases (B) and (C), substantial recovery was observed within 10 min after initial suppression. We did not observe any correlation between the asymmetry in suppression and the sequence of

Department of Biological Sciences, Columbia University, New York, NY 10027.

*To whom correspondence should be addressed.